Science Advances
AAAS

advances.sciencemag.org/cgi/content/full/6/35/eaaz4796/DC1

# Supplementary Materials for

## Disruption in *ACTL7A* causes acrosomal ultrastructural defects in human and mouse sperm as a novel male factor inducing early embryonic arrest

Aijie Xin, Ronggui Qu, Guowu Chen, Ling Zhang, Junling Chen, Chengqiu Tao, Jing Fu, Jianan Tang, Yanfei Ru, Ying Chen, Xiandong Peng, Huijuan Shi*, Feng Zhang*, Xiaoxi Sun*

*Corresponding author. Email: xiaoxi_sun@aliyun.com (X.S.); zhangfeng@fudan.edu.cn (F.Z.); shihuijuan2011@163.com (H.S.)

Published 28 August 2020, *Sci. Adv.* **6**, eaaz4796 (2020)
DOI: 10.1126/sciadv.aaz4796

**The PDF file includes:**



**Other Supplementary Material for this manuscript includes the following:**

(available at advances.sciencemag.org/cgi/content/full/6/35/eaaz4796/DC1)

## Supplementary Materials

## Supplementary figures

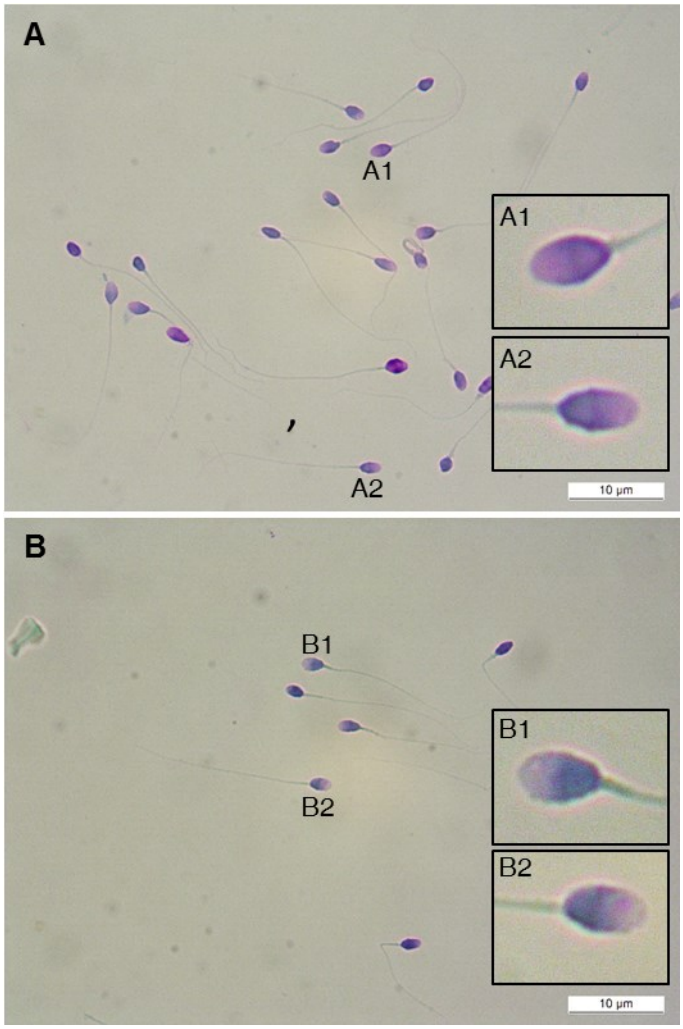


**Figure S1. Sperm morphology of the affected brothers under light microscopy.** Sperm samples of brother 1 (A) and brother 2 (B) were spread over slides and dried at room temperature, fixed in 95% ethanol for Papanicolaou stain. Spermatozoa were then scored by ×100 oil-immersion bright-field objective according to the standard of the fifth edition of the WHO guidelines. A1, A2, B1 and B2 correspond to enlarged spermatozoa with normal morphology. Photo credit: Aijie Xin, Fudan University.

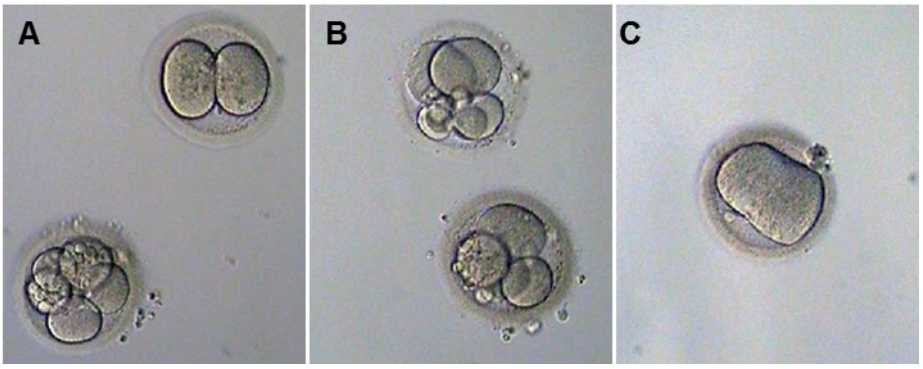


**Figure S2. Day 3 embryos of one brother couple by ICSI treatment.**

Seven oocytes were fertilized with sperm of brother 1 by ICSI. The images A, B and C showed the Day 3 embryos. They all arrested at 2-cell, 4-cell or 5-cell stage. Photo credit: Jing Fu, Fudan University.

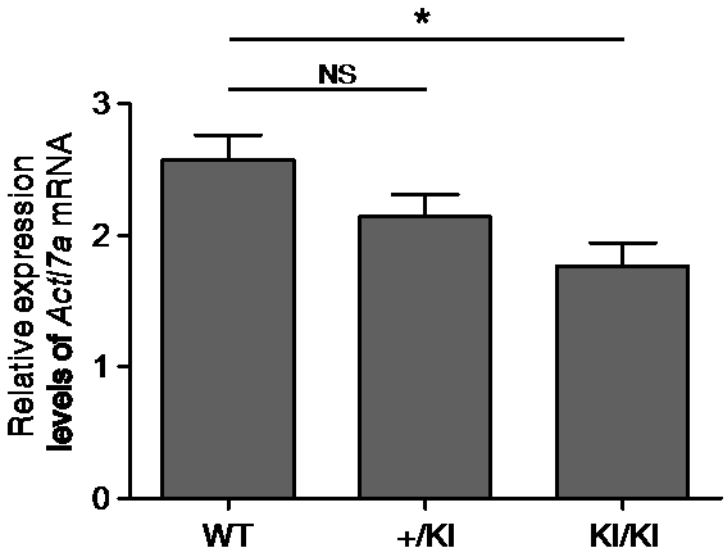


**Figure S3. *Actl7a* expression was significantly decreased in testes of *Actl7a*$^{KI/KI}$ mice.**

The relative mRNA level of *Actl7a* in testes of the *Actl7a*-mutated mice (*Actl7a*$^{KI/KI}$) was significantly decreased by approximately 30% analyzed by one-way ANOVA. Nine testicular samples of each genotype group were used for biological replicates. Three duplicates of each sample were performed by RT-qPCR assays. *Gapdh* served as a reference gene. * $P < 0.05$; NS, not significant. Data are represented as the mean ± SEM.

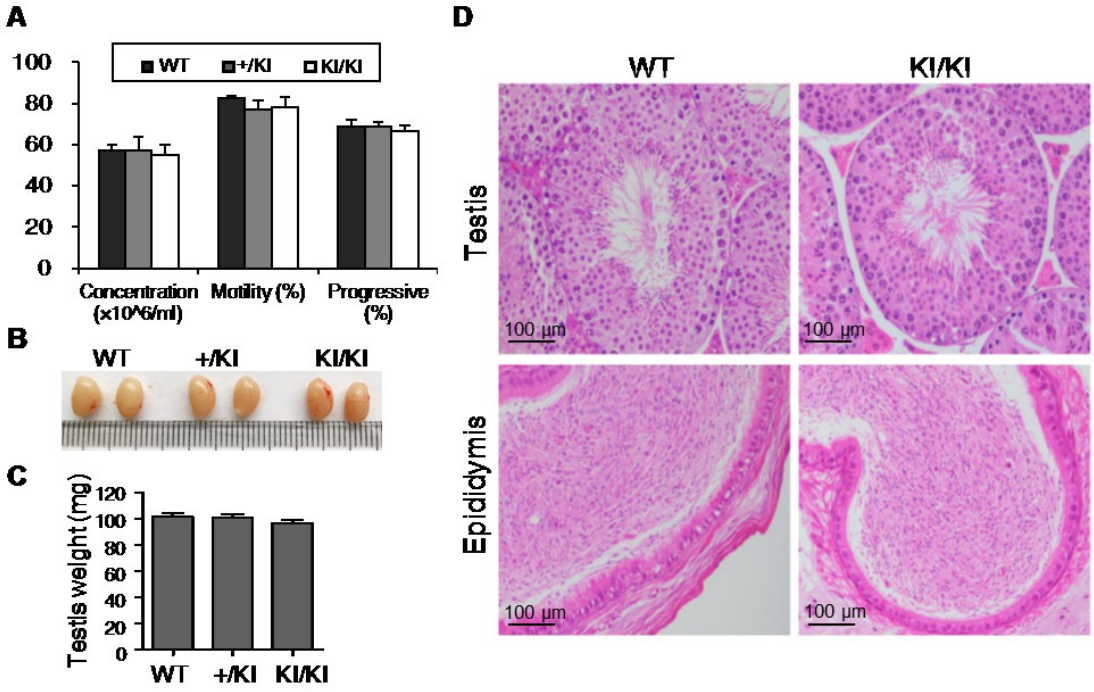


**Figure S4. Homozygous knock-in mutation in *Actl7a* has no obvious effect on sperm motility, testis weight or development of reproductive system in mice.**

(A) Motility parameters of spermatozoa in the cauda region were compared among the mice with wile-type (WT), *Actl7a*$^{+/KI}$ or *Actl7a*$^{KI/KI}$ genotypes. Three sperm samples in each group were used for biological replicates. The semen parameters showed no significant difference among the three genotypes. Data are represented as the mean ± SEM. (B) The morpha and size of testes from *Actl7a*$^{KI/KI}$ mice showed no major change compared to those of WT and *Actl7a*$^{+/KI}$ mice. (C) Testis weight presented no significant difference among WT, *Actl7a*$^{+/KI}$ and *Actl7a*$^{KI/KI}$ mice. Five mice in each group were used for biological replicates. Data are represented as the mean ± SEM. (D) H&E stained cross sections of testis and cauda epididymis of WT and *Actl7a*$^{KI/KI}$ mice. The histomorphology of seminiferous tubules and caudal epididymis in *Actl7a*$^{KI/KI}$ mice appeared similar to those of the WT male mice. Scale bars: 100 μm. Photo credit: Aijie Xin, Fudan University.

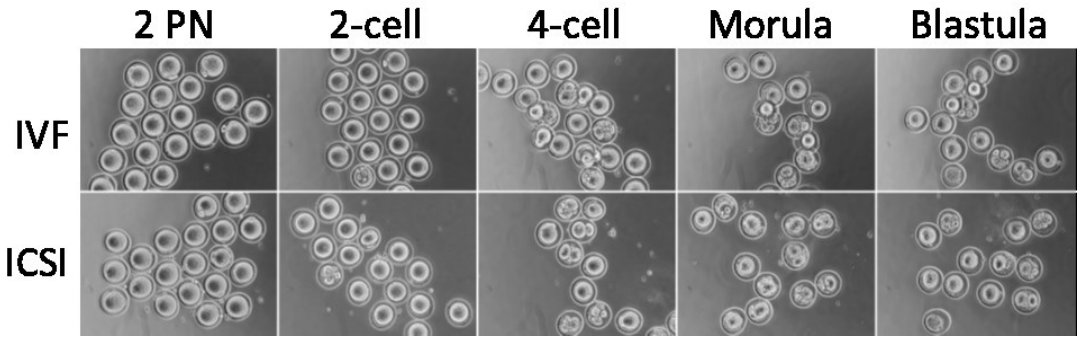


**Figure S5. Spermatozoa from the *Actl7a*$^{KI/KI}$ mice failed to fertilize normal mouse oocytes by IVF and ICSI.** Photo credit: Aijie Xin, Fudan University.

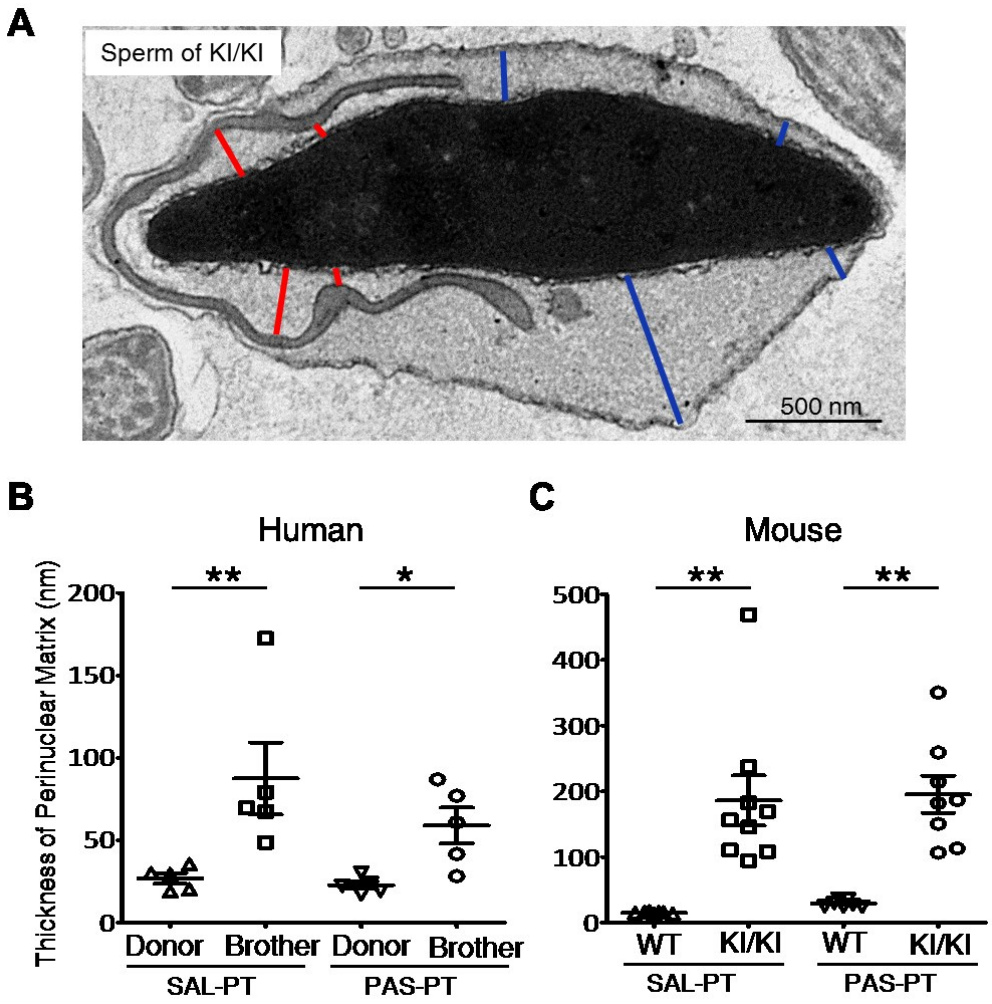


**Figure S6. The thickness of perinuclear theca in brother and mouse sperm with homozygous *Actl7a* mutation.**

(A) Measurement of PT thickness. The four red lines are the measuring area of the subacrosomal layer of the perinuclear theca (SAL-PT); the four blue lines are the measuring area of the postacrosomal sheath of the perinuclear theca (PAS-PT). Taken the average value as the thickness of SAL-PT and PAS-PT. (B) Significant increase of the thickness of SAL-PT and PAS-PT in brother sperm. (C) Significant increase of the thickness of SAL-PT and PAS-PT in sperm from the male mice carrying homozygous *Actl7a* mutation. Photo credit: Aijie Xin, Fudan University.

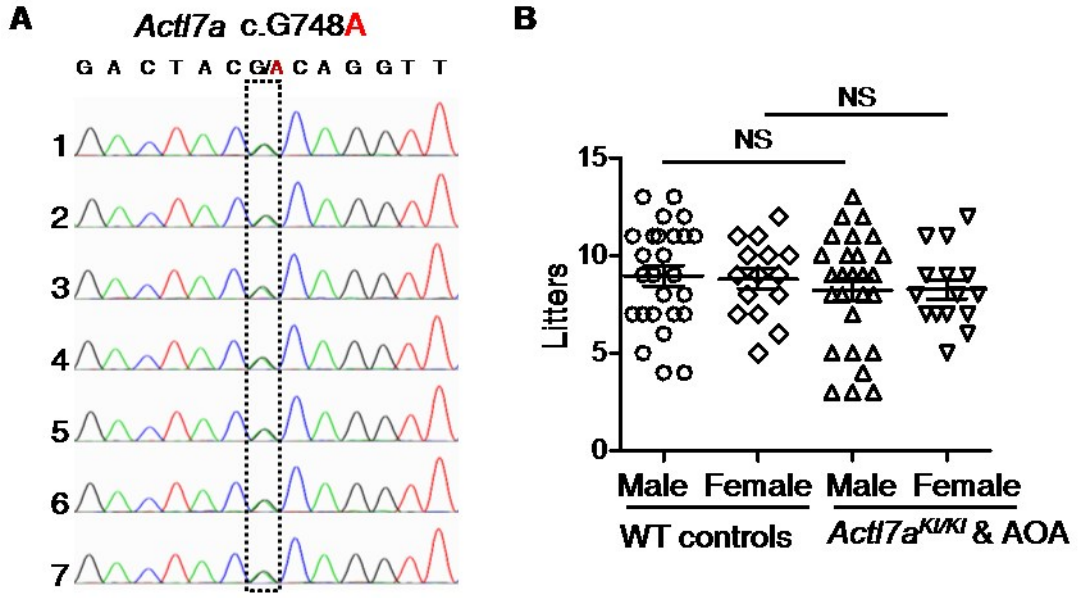


**Figure S7. Genotyping and fertility of the offspring from *Actl7a*$^{KI/KI}$ mice.**

(A) The number represented the mice marked with dotted circle in figure 5D. Dotted rectangle indicate the position of *Actl7a* point mutation. (B) The fertility rate presented no significant difference between the offspring of the *Actl7a*$^{KI/KI}$ male mice and the wild-type (WT) controls. Male, n=5; Female, n=5. Two-tailed Student's *t* test; NS, not significant.

## Supplementary tables

**Table S1. Semen parameters of the two brothers affected by a homozygous *ACTL7A* mutation.**

| | Brother 1 | Brother 2 | Low reference limits of WHO criteria |
|---|---|---|---|
| Age | 29 | 28 | / |
| Semen volume (ml) | 1.8 | 7.0 | 1.5 (1.4–1.7) |
| Sperm concentration ($10^6$/ml) | 325 | 162 | 15 (12–16) |
| Total sperm ($10^6$) | 585 | 1134 | 39 (33–46) |
| Progressive motility (PR, %) | 54.7 | 68.4 | 32 (31–34) |
| Total motility (PR+NP, %) | 76.6 | 78.1 | 40 (38–42) |

**Table S2. The ART history of two affected couples before the genetic diagnosis of this study.**

| | Brother 1 | | | | Brother 2 | | | |
|---|---|---|---|---|---|---|---|---|
| Cycle ID | 1 | 2 | 3 | 4 | 1 | 2 | 3 | |
| No. of oocytes retrieved | 21 | 19 | 17 | 19 | 5 | 8 | 7 | |
| No. of mature oocytes (M II) | 17 | 17 | 14 | 19 | 4 | 6 | 5 | |
| Method of ART | Later-ICSI | ICSI | ICSI | DIVF | DIVF | IVF | ICSI | DIVF |
| No. of fertilization (2PN) | 9 | 9 | 7 | 6 | 17 | 0 | 3 | 5 |
| No. of embryo for transfer* | 0 | 0 | 0 | 6 | 11 | 0 | 0 | 4 |
| No. of good quality embryo† | 0 | 0 | 0 | 6 | 9 | 0 | 0 | 3 |
| Live birth | 0 | 0 | 0 | 0 | 2 | 0 | 0 | 1 |

* Embryo for transfer: Grade 2, ≥5 cells.

† Good quality embryos: Grade 1, ≥7-8 cells.

Abbreviations: ICSI, intracytoplasmic sperm injection; IVF, in vitro fertilization; DIVF, donor sperm in vitro fertilization.

**Table S3. The development rate of mouse embryos in different development stages after AOA.**

| | WT | KI/KI | $SrCl_2$ | $SrCl_2$+ KI/KI |
|---|---|---|---|---|
| 2 PN (%)* | 93.0 ± 3.9 | 0 | 93.3±4.0 | 64.4 ± 3.2 |
| 2-cell (%) † | 86.0 ± 14 | / | 91.4 ± 2.5 | 94.0 ± 4.3 |
| 4-cell (%) † | 84.0 ± 8.0 | / | 71.8 ± 3.1 | 84.0 ± 6.4 |
| Morula (%) † | 84.0 ± 8.0 | / | 71.8 ± 3.1 | 89.8 ± 3.7 |
| Blastula (%) † | 79.8 ± 3.9 | / | 29.9 ± 3.3 | 49.0 ± 7.4 |

* Percentages of 2PN were calculated from the total number of injected oocytes.

† Percentages of 2-cell embryos to blastula were calculated from 2PN.

**Table S4. Sequence of single-guide RNA (sgRNA) and the single-stranded oligonucleotide (ssODN).**

| Material | Sequence (5′ - 3′) |
|---|---|
| sgRNA | ACGGGGAGGCTAGACTACGC |
| ssODN | TATGAGGGTTATCCTTTGCCCAGCATCACGGGGAGGCTAGACTACACAGGT |
| | TCTGACCTAACGACCTACCTGATGAACCTGATGAACAA |

Note: The protospacer adjacent motif (PAM) sequence is shown in red, and the mutated target is shown in blue.

## Supplementary movies

**Movies S1 to 4. The embryonic development from day 0 to day 3 following ICSI with AOA in the case of brother 2 and his wife.**